

Blockage-Aware Multi-RIS WSR Maximization via Per-RIS Indexed Synchronization Sequences and Closed-Form Riemannian Updates

Sehyun Ryu and Hyun Jong Yang, *Senior Member, IEEE*

Abstract—Millimeter-wave (mmWave) multi-user MIMO systems are highly vulnerable to link blockage, and reconfigurable intelligent surfaces (RISs) have been proposed to establish alternative propagation paths. However, RIS-assisted links may themselves be intermittently blocked, while most existing works implicitly assume ideal RIS availability. We propose a lightweight blockage-aware optimization framework for multi-RIS mmWave systems. The base station transmits short per-RIS indexed synchronization signals, enabling each user to identify its unblocked RIS panels via a low-complexity energy detection test under multipath and multi-user interference. Based on the detected feasible RIS sets, we jointly optimize the BS precoder and RIS phases using a closed-form Riemannian phase alignment (CRPA) algorithm. CRPA yields unit-modulus-preserving closed-form updates without projection or line search, supports discrete phase constraints, and ensures monotone ascent for continuous-phase RISs. Simulation results demonstrate reliable per-RIS blockage detection, competitive WSR performance, and faster convergence than existing multi-RIS baselines.

Index Terms—Reconfigurable Intelligent Surface (RIS), Multi-RIS, Blockage Detection, Weighted Sum Rate Maximization, Riemannian Optimization.

I. INTRODUCTION

Millimeter-wave (mmWave) communications have been highlighted as a key research direction for future wireless systems [1], and current standards are moving toward progressively higher frequency bands. At such frequencies, diffraction is weak and communication relies heavily on line-of-sight propagation, making mmWave links highly vulnerable to blockage. To establish alternative propagation paths and enhance coverage, reconfigurable intelligent surfaces (RISs) have been proposed [2]. A metasurface-based RIS operates as a programmable phase shifter that controls the phase of incident signals, thereby enabling reconfiguration of the wireless propagation environment [3].

Extensive research has investigated the joint optimization of the downlink precoder and RIS phase matrix under various objectives. Early works focused on minimizing the total transmit power [2], followed by designs incorporating quality-of-service (QoS) balancing among users [4]. In addition, [5]

S. Ryu is with the Department of Electrical Engineering, Pohang University of Science and Technology (POSTECH), Pohang, Republic of Korea, and is also with the Institute of New Media and Communications, Seoul National University (SNU), Seoul, Republic of Korea.

H. J. Yang is the corresponding author and is with the Department of Electrical and Computer Engineering and the Institute of New Media and Communications, Seoul National University (SNU), Seoul, Republic of Korea (e-mail: hjyang@snu.ac.kr).

studied the maximization of received power through a joint optimization of beamforming, RIS phase shifts, and the position and orientation of the RIS. More recently, weighted sum-rate (WSR) maximization in multi-user scenarios has become a central research direction, including studies for MU-MISO systems [6] and mmWave systems where fractional programming and alternating optimization were applied [7]. Research on single-RIS systems has also been extended to multi-RIS architectures. For example, [8] investigated channel estimation and beamforming in double-RIS systems, while [9] studied phase optimization to maximize WSR in MU-MISO multi-RIS scenarios. A Riemannian manifold optimization approach for jointly optimizing the precoder and phase shifts in MU-MIMO double-RIS systems was proposed in [10]. Furthermore, [11] addressed channel modeling in MU-MISO multi-RIS systems and introduced a beamforming optimization method based on auxiliary variables.

Since RIS was originally proposed as a means to overcome blockage, several studies have also considered cases where the RIS-assisted paths themselves are blocked. Early work in [12] investigated beamformer optimization under random link blockages across different blockage combinations. Subsequent studies primarily relied on statistical or learning-based assumptions about blockage. For example, [13] employed stochastic learning to capture blockage patterns and designed beamforming schemes under uncertain path blockages, while [14] proposed a learning-based beamforming method for RIS-aided mmWave systems under random blockages. More recently, [15] optimized the precoder and phase shifts to maximize WSR in mmWave massive MIMO systems with mobile RIS under known blockage conditions, but without addressing how to detect blockage in practice. In contrast, [16] proposed a binary Neyman–Pearson (NP) detection method to sense and optimize blockage in a single-RIS system. However, in multi-RIS scenarios, the superposition of multipath components from different RIS panels makes per-RIS signal isolation difficult, rendering NP-style binary detection infeasible.

In this paper, we consider deterministic blockage-aware WSR maximization in a multi-RIS mmWave system. The base station (BS) transmits short per-RIS indexed synchronization sequences toward different RIS panels, and each user equipment (UE) measures the received power per index to identify its unblocked RIS panels via a simple energy detection test. While prior art has exploited RIS-indexed synchronization mainly for uplink random access or panel identification [17], we repurpose such sequences for downlink per-RIS blockage

detection and RIS set selection. Based on the detected feasible RIS sets, we jointly optimize the BS precoder and RIS phases using a closed-form Riemannian phase alignment (CRPA) scheme. CRPA admits unit-modulus-preserving closed-form updates on the complex-circle manifold, ensuring feasibility without projection and guaranteeing monotone WSR ascent for continuous-phase RISs without line search.

We assume quasi-static channels with perfect instantaneous CSI and focus on deterministic blockage-aware WSR maximization based on the detected RIS sets. This scope allows us to isolate the impact of per-RIS blockage detection and RIS phase optimization on the achievable WSR performance in multi-RIS mmWave systems.

Contributions: 1) We propose a simple UE-side energy detector using per-RIS indexed synchronization sequences to identify downlink blockages and estimate the active RIS set with minimal overhead in multi-RIS mmWave systems. 2) We develop a CRPA algorithm for multi-RIS WSR maximization that yields elementwise unit-modulus-preserving updates without projection or line search and guarantees monotone WSR ascent for continuous-phase RISs. 3) We present simulation results demonstrating reliable per-RIS blockage detection and faster WSR convergence with competitive performance over existing multi-RIS baselines.

II. SYSTEM MODEL AND PROBLEM FORMULATION

We consider a downlink mmWave MU-MIMO multi-RIS system with K users and M RIS panels, where RIS- i has N_i reflecting elements (Fig. 1). Each RIS is a passive phase-only surface with constant-modulus reflection coefficients. The BS has N_t antennas, and UE- k has $N_{r,k}$ antennas.

We assume quasi-static channels with perfect instantaneous CSI and focus on a single-carrier (per-subcarrier) OFDM downlink model. Each pilot symbol is transmitted with a cyclic prefix (CP) longer than the maximum delay spread so that the cyclic correlation of indexed synchronization sequences is preserved under multipath (details in Section III).

Let $\mathcal{R}_k \subseteq \{1, \dots, M\}$ denote the *ground-truth* set of RIS panels whose cascaded BS \rightarrow RIS- i \rightarrow UE- k path is unblocked for UE- k . Based on downlink synchronization, UE- k forms an estimate $\widehat{\mathcal{R}}_k$. Throughout the paper, \mathcal{R}_k and $\widehat{\mathcal{R}}_k$ are distinguished: \mathcal{R}_k is the unknown true set, while $\widehat{\mathcal{R}}_k$ is its detected counterpart used for optimization.

We decouple the overall design into: (i) estimating $\widehat{\mathcal{R}}_k$ via per-RIS indexed synchronization, and (ii) maximizing the WSR based on $\widehat{\mathcal{R}}_k$.

A. Per-RIS Blockage Detection

Each RIS panel is tagged by a distinct cyclic shift of a Zadoff-Chu (ZC) synchronization sequence, as detailed in Section III. Let $Z_{k,i}$ denote the matched-filter output at UE- k corresponding to the ZC index assigned to RIS- i .

The estimated feasible RIS set is obtained via a per-index energy test

$$\widehat{\mathcal{R}}_k = \{ i \in \{1, \dots, M\} \mid |Z_{k,i}|^2 \geq \tau_i \}, \quad (1)$$

where $\tau_i \geq 0$ is the detection threshold for panel i .

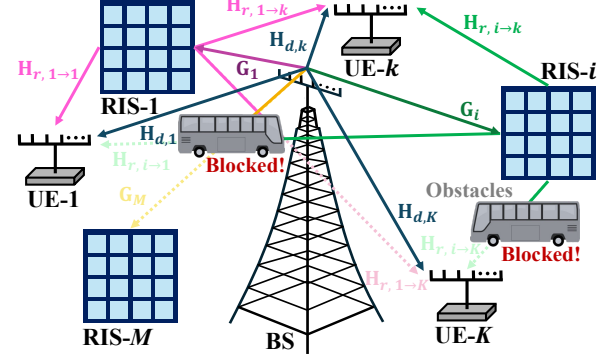


Fig. 1: Multi-RIS aided mmWave MU-MIMO downlink system.

Detection accuracy is measured by the Jaccard index

$$\mathcal{J}_k = \frac{|\widehat{\mathcal{R}}_k \cap \mathcal{R}_k|}{|\widehat{\mathcal{R}}_k \cup \mathcal{R}_k|}, \quad (2)$$

which we aim to maximize by designing the thresholds $\tau = (\tau_1, \dots, \tau_M)$.

B. WSR Maximization

For RIS- i , let $u_i \in \mathbb{C}^{N_i}$ denote its reflection coefficient vector with $||u_i||_m = 1, \forall m$. The effective downlink channel to UE- k is

$$\mathbf{H}_{k,\text{eff}} = \mathbf{H}_{d,k} + \sum_{i \in \widehat{\mathcal{R}}_k} \mathbf{H}_{r,i \rightarrow k} \text{diag}(u_i) \mathbf{G}_i, \quad (3)$$

where $\mathbf{H}_{d,k}$, \mathbf{G}_i , and $\mathbf{H}_{r,i \rightarrow k}$ denote the direct BS-UE, BS-RIS- i , and RIS- i -UE- k channels.

With a linear precoder $\mathbf{F} = [\mathbf{f}_1, \dots, \mathbf{f}_K] \in \mathbb{C}^{N_t \times K}$ satisfying $\|\mathbf{F}\|_F^2 \leq P$, the received signal at UE- k is

$$\mathbf{y}_k = \mathbf{H}_{k,\text{eff}} \mathbf{F} \mathbf{s} + \mathbf{n}_k, \quad (4)$$

where $\mathbf{s} \in \mathbb{C}^K$ and $\mathbf{n}_k \sim \mathcal{CN}(0, \sigma^2 \mathbf{I}_{N_{r,k}})$.

We maximize the WSR as

$$\begin{aligned} & \max_{\mathbf{F}, \{u_i\}} \sum_{k=1}^K \omega_k \log \det(\mathbf{I}_{N_{r,k}} + \mathbf{R}_k^{-1} \mathbf{H}_{k,\text{eff}} \mathbf{f}_k \mathbf{f}_k^H \mathbf{H}_{k,\text{eff}}^H) \\ & \text{s.t. } \|\mathbf{F}\|_F^2 \leq P, \quad ||u_i||_m = 1, \end{aligned} \quad (5)$$

where $\mathbf{R}_k = \sigma^2 \mathbf{I}_{N_{r,k}} + \sum_{j \neq k} \mathbf{H}_{k,\text{eff}} \mathbf{f}_j \mathbf{f}_j^H \mathbf{H}_{k,\text{eff}}^H$.

III. PER-RIS INDEXED SYNCHRONIZATION AND ENERGY-BASED BLOCKAGE DETECTION

A. Indexed Zadoff-Chu pilots with CP

RIS- i is tagged by a cyclic shift of a root ZC sequence of length ℓ :

$$s[n] = \exp\left(-j \frac{\pi q n (n+1)}{\ell}\right), \quad (6)$$

$$s_i[n] \triangleq s[(n+i) \bmod \ell], \quad i = 0, \dots, M-1. \quad (7)$$

If $M \leq \ell$, all RISs are indexed within one pilot symbol; otherwise we use $T_p = \lceil M/\ell \rceil$ pilot symbols (or multiple ZC roots). We assume an OFDM pilot with a CP longer than the maximum delay spread, so that after CP removal the multipath convolution becomes circular over the ℓ useful samples, preserving the near-orthogonality among cyclic shifts up to small residual leakage.

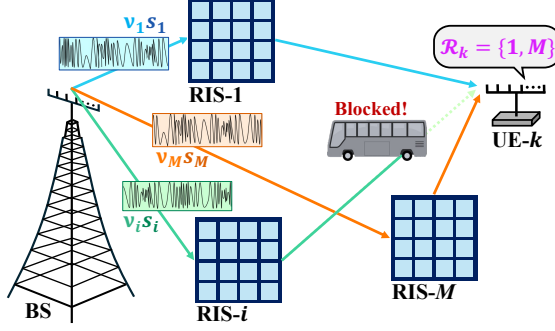


Fig. 2: Per-RIS synchronization using indexed Zadoff–Chu sequences.

B. Pilot transmission and matched filtering

During a sensing interval, the BS transmits a superposition of indexed pilots:

$$\mathbf{x}[n] = \sum_{i=1}^M \mathbf{v}_i s_i[n], \quad \sum_{i=1}^M \|\mathbf{v}_i\|_2^2 \leq P_{\text{pilot}}, \quad (8)$$

with equal power $\|\mathbf{v}_i\|_2^2 = P_{\text{pilot}}/M$. This choice is made for simplicity and uniform probing across RISs, and to avoid introducing additional design variables into the sensing stage. Each RIS uses a known sensing state $u_i^{(0)}$ (e.g., all-pass).

After CP removal, the received signal at UE- k is

$$\mathbf{y}_k[n] = \sum_{i=1}^M \mathbf{H}_{k,i}^{\text{eff}} \mathbf{v}_i s_i[n] + \mathbf{n}_k[n], \quad (9)$$

where $\mathbf{n}_k[n] \sim \mathcal{CN}(\mathbf{0}, \sigma^2 \mathbf{I})$. Since $\mathbf{H}_{k,i}^{\text{eff}}$ is unknown during sensing, UE- k applies a fixed combiner $\tilde{y}_k[n] \triangleq \mathbf{w}_k^H \mathbf{y}_k[n]$ with $\|\mathbf{w}_k\|_2 = 1$. The matched-filter statistic for RIS- i is

$$Z_{k,i} \triangleq \sum_{n=0}^{\ell-1} s_i^*[n] \tilde{y}_k[n], \quad (10)$$

which consists of the desired RIS- i contribution plus residual multi-RIS leakage and noise due to imperfect cyclic orthogonality under multipath.

C. Energy-based per-RIS detection

Blockage is decided via a per-index energy test

$$|Z_{k,i}|^2 \stackrel{\mathcal{H}_U}{\gtrless} \tau_i. \quad (11)$$

Under \mathcal{H}_B , the desired term is absent and only residual leakage and noise remain. Since the aggregate disturbance is a weighted sum of many weak interference and noise components, we adopt a second-order-matched Gaussian approximation based on the central limit effect and model

$$Z_{k,i} | \mathcal{H}_B \approx \mathcal{CN}(0, \sigma_{k,i}^2 \ell). \quad (12)$$

Fixing a false-alarm target α_i yields the NP threshold

$$\tau_i = -\sigma_{k,i}^2 \ell \ln \alpha_i. \quad (13)$$

Disturbance variance estimation: UE- k estimates $\sigma_{k,i}^2$ from pilot-only resources where the i -th indexed pilot is absent (e.g., guard or idle REs). An unbiased estimator is

$$\hat{\sigma}_{k,i}^2 = \frac{1}{T_g \ell} \sum_{t=1}^{T_g} |Z_{k,i}^{(g)}(t)|^2, \quad (14)$$

where T_g is the number of pilot-only resources used for variance estimation. Finally, the detected RIS set is

$$\hat{\mathcal{R}}_k = \left\{ i \in \{1, \dots, M\} \mid |Z_{k,i}|^2 \geq \tau_i \right\}. \quad (15)$$

D. Overhead and complexity

A pilot symbol supports $M \leq \ell$ RIS indices; otherwise, $T_p = \lceil M/\ell \rceil$ pilot symbols are used. Per UE, matched filtering and circular correlation cost $O(N_r \ell)$ and $O(\ell \log \ell)$, respectively, assuming an FFT-based implementation. These operations are consistent with standard receiver processing and can be executed within the normal pilot processing time.

IV. CLOSED-FORM RIEMANNIAN PHASE ALIGNMENT (CRPA) FOR MULTI-RIS WSR MAXIMIZATION

The WSR maximization in (5) is nonconvex due to the coupled precoder–RIS variables and unit-modulus constraints. Using the standard WSR–WMMSE equivalence [18], we introduce per-user linear receivers \mathbf{U}_k and weights \mathbf{W}_k (single stream $d_k=1$) and obtain the equivalent problem

$$\begin{aligned} & \min_{\mathbf{F}, \{\mathbf{U}_k, \mathbf{W}_k\}, \{u_i\}} \sum_{k=1}^K \left(\text{Tr}(\mathbf{W}_k \mathbf{E}_k) - \log \det \mathbf{W}_k \right) \\ & \text{s.t. } \|\mathbf{F}\|_F^2 \leq P, \quad |[u_i]_m| = 1. \end{aligned} \quad (16)$$

We adopt a block-coordinate scheme that updates $\{\mathbf{U}_k, \mathbf{W}_k\}$, \mathbf{F} , and $\{u_i\}$ sequentially.

(A) Receiver and weight. For fixed $(\mathbf{F}, \{u_i\})$, the closed-form updates are

$$\mathbf{U}_k \leftarrow (\mathbf{H}_{k,\text{eff}} \mathbf{F} \mathbf{F}^H \mathbf{H}_{k,\text{eff}}^H + \sigma^2 \mathbf{I})^{-1} \mathbf{H}_{k,\text{eff}} \mathbf{f}_k, \quad (17)$$

$$\mathbf{W}_k \leftarrow \mathbf{E}_k^{-1}. \quad (18)$$

(B) Precoder. For fixed $(\{\mathbf{U}_k, \mathbf{W}_k\}, \{u_i\})$, define

$$\mathbf{A} \triangleq \sum_{k=1}^K \mathbf{H}_{k,\text{eff}}^H \mathbf{U}_k \mathbf{W}_k \mathbf{U}_k^H \mathbf{H}_{k,\text{eff}}, \quad (19)$$

$$\mathbf{B} \triangleq [\mathbf{H}_{1,\text{eff}}^H \mathbf{U}_1 \mathbf{W}_1, \dots, \mathbf{H}_{K,\text{eff}}^H \mathbf{U}_K \mathbf{W}_K]. \quad (20)$$

Then

$$\mathbf{F} \leftarrow (\mathbf{A} + \lambda \mathbf{I})^{-1} \mathbf{B}, \quad (21)$$

where $\lambda \geq 0$ is chosen by bisection so that $\|\mathbf{F}\|_F^2 = P$.

(C) RIS phases (CRPA). Let $f(\{u_i\})$ denote the value function obtained after substituting the closed-form $\{\mathbf{U}_k, \mathbf{W}_k\}$ and \mathbf{F} into (16). Using Wirtinger calculus [19], compute the conjugate gradient $g_i^{(t)} = \partial f / \partial u_i^* |_{u=u^{(t)}}$ (given in (24)). With a stepsize $L_i > 0$ (selected by backtracking), CRPA updates u_i via the following elementwise phase-alignment rule:

$$u_i^{(t+1)} = \exp(j \arg(c_i^{(t)})), \quad c_i^{(t)} \triangleq g_i^{(t)} + L_i u_i^{(t)}, \quad (22)$$

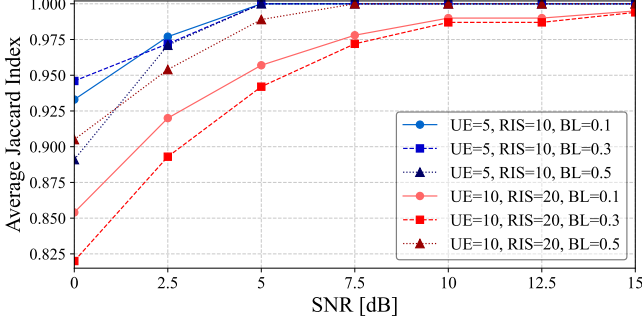


Fig. 3: Jaccard index for blockage detection versus SNR under $\alpha = 10^{-3}$ with indexed Zadoff–Chu pilots ($\ell=63$, $L_{\text{cp}}=8$).

which preserves $|\{u_i\}_m| = 1$ by construction and yields a monotone ascent of f for continuous-phase RISs.

Discrete phase shifts: With b -bit quantization, phases are restricted to $\Theta_b \triangleq \{0, \frac{2\pi}{2^b}, \dots, \frac{2\pi(2^b-1)}{2^b}\}$. After (22), we update

$$u_i^{(t+1)} \leftarrow \exp(j Q_b(\arg(c_i^{(t)}))), \quad (23)$$

where $Q_b(\cdot)$ denotes nearest-neighbor quantization onto Θ_b .

Gradient computation: Let $\mathbf{Q} = \mathbf{F}\mathbf{F}^H$, $\Psi_k = \mathbf{U}_k \mathbf{W}_k \mathbf{U}_k^H$, $\mathbf{C}_k = \mathbf{U}_k \mathbf{W}_k \mathbf{f}_k^H$, and $\mathcal{K}_i = \{k : i \in \widehat{\mathcal{R}}_k\}$. Then

$$g_i = \sum_{k \in \mathcal{K}_i} \text{diag}\left(\mathbf{H}_{r,i \rightarrow k}^H (\Psi_k \mathbf{H}_{k,\text{eff}} \mathbf{Q} - \mathbf{C}_k) \mathbf{G}_i^H\right). \quad (24)$$

V. EXPERIMENTAL RESULTS

We evaluate the proposed per-RIS blockage detection and CRPA-based WSR optimization via Monte Carlo simulations under a unified mmWave MU–MIMO multi-RIS model.

A. Simulation setup

Carrier/arrays: We consider a mmWave system at carrier frequency $f_c = 28$ GHz and a narrowband per-subcarrier equivalent channel model for WSR evaluation. The BS employs an $N_t = 16$ uniform linear array (ULA) and each UE employs an $N_r = 4$ ULA with inter-element spacing $\lambda/2$, where λ denotes the carrier wavelength. Each RIS is modeled as a uniform planar array (UPA) with $N_i=16$ reflecting elements arranged on a 4×4 grid and $\lambda/2$ inter-element spacing in both dimensions, with passive phase-only control. Unless stated otherwise, WSR results use 2-bit RIS phase quantization.

Geometry: The BS is located at the origin. RIS- i is placed at a random azimuth angle with distance $d_{\text{BR},i} \sim \mathcal{U}[15, 40]$ m, and UE- k is placed with $d_{\text{BU},k} \sim \mathcal{U}[10, 50]$ m. Each UE has at least one RIS within $d_{\text{RU},\text{max}} = 15$ m; otherwise, its location is redrawn.

Channel/blockage: Each link $\mathbf{H}_{d,k}$, \mathbf{G}_i , and $\mathbf{H}_{r,i \rightarrow k}$ follows Rician fading with Rician factor $K_R = 5$,

$$\mathbf{H} = \sqrt{\frac{K_R}{K_R+1}} \mathbf{H}^{\text{LoS}} + \sqrt{\frac{1}{K_R+1}} \mathbf{H}^{\text{NLoS}}, \quad (25)$$

with geometry-based LoS steering and i.i.d. Rayleigh NLoS. Distance-dependent pathloss and noise variance σ^2 are applied. Each UE–RIS cascaded path is independently blocked with probability p_{blk} , defining the true set \mathcal{R}_k .

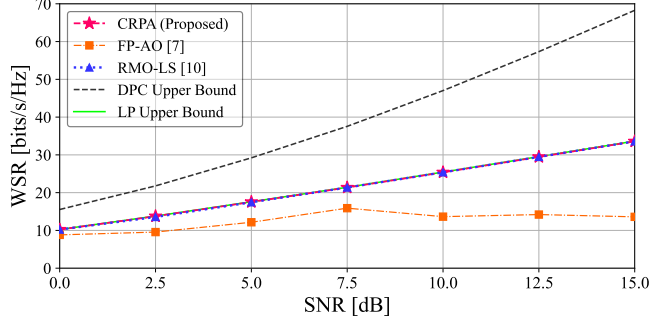


Fig. 4: WSR versus SNR for $K=5$, $M=10$, and $p_{\text{blk}}=0.1$ under 2-bit RIS phase quantization with perfect blockage detection.

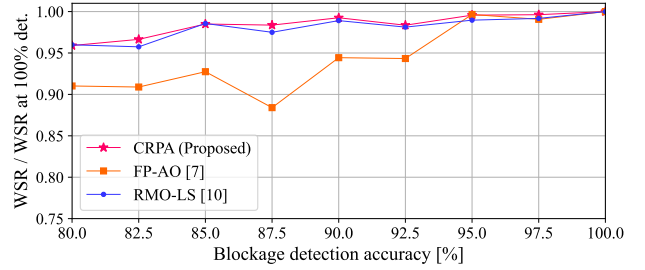


Fig. 5: Normalized WSR versus blockage-detection accuracy for $K=5$, $M=10$, and $p_{\text{blk}}=0.1$ with 2-bit RIS phase quantization.

Sensing: Blockage detection uses indexed ZC pilots with $(\ell, q) = (63, 25)$ and CP length $L_{\text{cp}} = 8$. Each RIS applies the all-pass state $u_i^{(0)}$ during sensing. Thresholds follow the interference-aware NP rule in Section III.

Monte Carlo: Each point is averaged over $N_{\text{MC}} = 100$ realizations. For detection-error sensitivity, $\widehat{\mathcal{R}}_k$ is synthetically perturbed to target accuracies (80–100%) with false negatives, consistent with conservative false-positive suppression; optimization is performed using $\widehat{\mathcal{R}}_k$, and WSR is evaluated on the true \mathcal{R}_k .

B. Performance of Per-RIS Indexed Blockage Detection

We set $\alpha = 10^{-3}$. Fig. 3 shows the Jaccard index \mathcal{J}_k averaged over UEs and Monte Carlo drops for $(K, M) = (5, 10)$ and $(10, 20)$. The proposed detector achieves high set-recovery accuracy over a wide SNR range under CP-assisted multipath and interference-aware thresholding.

C. WSR Performance with 2-bit Quantized RIS Phases

Given $\{\widehat{\mathcal{R}}_k\}$, we evaluate WSR under 2-bit RIS phases, i.e., $\Theta_2 = \{0, \frac{\pi}{2}, \pi, \frac{3\pi}{2}\}$. CRPA applies the nearest-neighbor quantizer (23) after each closed-form phase-alignment step. We use equal weights $\omega_k = 1$. Baselines are **CRPA (Proposed)**, **FP-AO** [7], **RMO-LS** [10], and the **LP/DPC upper bounds**. For fairness, RIS phases produced by each baseline are quantized elementwise to Θ_2 before objective evaluation. All methods run up to 200 iterations.

As shown in Fig. 4, CRPA achieves competitive WSR across the SNR range and approaches the LP upper bound. In contrast, FP-AO degrades noticeably under multi-RIS coupling and discrete phase constraints, while RMO-LS remains

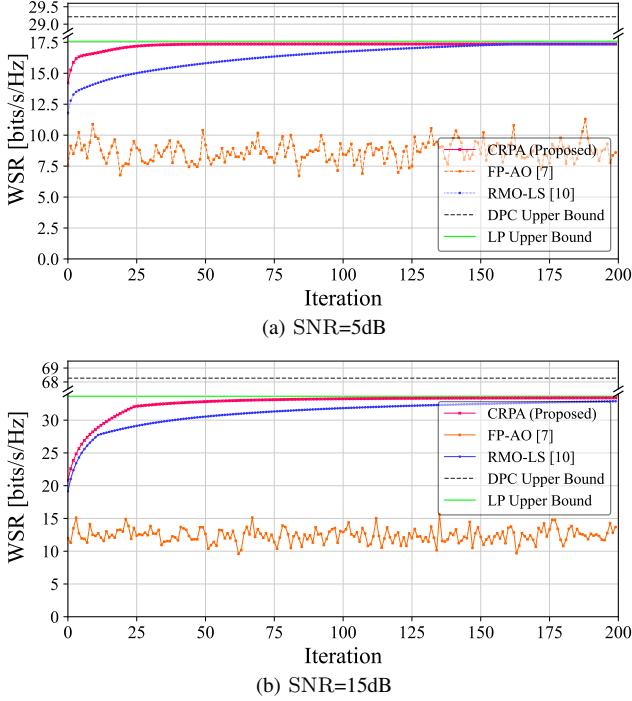


Fig. 6: WSR versus iteration count under 2-bit RIS phase quantization ($K=5$, $M=10$, $p_{blk}=0.1$).

competitive but converges more slowly. Fig. 5 shows that the overall WSR performance improves with increasing blockage-detection accuracy, underscoring the importance of accurate detection; a conservative threshold suppresses false positives to avoid wasting power on non-existent RIS paths, so that residual errors predominantly appear as false negatives.

D. Convergence and Complexity

Fig. 6 plots WSR versus iterations at $\text{SNR} = 5$ and 15 dB. CRPA uses backtracking (Section IV) to avoid WSR decreases caused by quantization and reaches 95% of its converged WSR in about 12 iterations on average, whereas RMO-LS requires substantially more iterations due to line searches. Per-iteration costs are dominated by receiver and precoder updates. For RIS updates, CRPA requires $O(\sum_i N_i)$ (plus elementwise quantization), while RMO-LS costs $O((1 + T_{ls}) \sum_i N_i)$ with empirically $T_{ls} \approx 35\text{--}45$. Thus, CRPA attains faster convergence with lower RIS-update cost under quantized phases.

VI. CONCLUSION

We proposed an end-to-end blockage-aware framework for multi-RIS-aided mmWave MU-MIMO systems. Using per-RIS indexed synchronization sequences, each UE can detect its unblocked RIS panels with minimal overhead. The resulting feasible sets are incorporated into a WSR maximization problem, solved by the proposed closed-form Riemannian phase alignment (CRPA) algorithm. CRPA preserves unit-modulus feasibility, supports discrete phase quantization, and guarantees monotone ascent for continuous-phase RISs without projection or line search. Simulation results demonstrate accurate per-RIS blockage detection and competitive WSR performance with faster convergence over existing baselines.

REFERENCES

- [1] T. S. Rappaport, Y. Xing, O. Kanhere, S. Ju, A. Madanayake, S. Mandal, A. Alkhateeb, and G. C. Trichopoulos, "Wireless communications and applications above 100 ghz: Opportunities and challenges for 6g and beyond," *IEEE Access*, vol. 7, pp. 78 729–78 757, 2019.
- [2] Q. Wu and R. Zhang, "Intelligent reflecting surface enhanced wireless network via joint active and passive beamforming," *IEEE Transactions on Wireless Communications*, vol. 18, no. 11, pp. 5394–5409, 2019.
- [3] W. Chen, L. Bai, W. Tang, S. Jin, W. X. Jiang, and T. J. Cui, "Angle-dependent phase shifter model for reconfigurable intelligent surfaces: Does the angle-reciprocity hold?" *IEEE Communications Letters*, vol. 24, no. 9, pp. 2060–2064, 2020.
- [4] R. Liu, M. Li, Q. Liu, and A. L. Swindlehurst, "Joint symbol-level precoding and reflecting designs for irs-enhanced mu-miso systems," *IEEE Transactions on Wireless Communications*, vol. 20, no. 2, pp. 798–811, 2021.
- [5] X. Cheng, Y. Lin, W. Shi, J. Li, C. Pan, F. Shu, Y. Wu, and J. Wang, "Joint optimization for ris-assisted wireless communications: From physical and electromagnetic perspectives," *IEEE Transactions on Communications*, vol. 70, no. 1, pp. 606–620, 2022.
- [6] H. Guo, Y.-C. Liang, J. Chen, and E. G. Larsson, "Weighted sum-rate maximization for reconfigurable intelligent surface aided wireless networks," *IEEE Transactions on Wireless Communications*, vol. 19, no. 5, pp. 3064–3076, 2020.
- [7] D. L. Dampahalage, K. B. S. Manosha, N. Rajatheva, and M. Latvala-Aho, "Weighted-sum-rate maximization for an reconfigurable intelligent surface aided vehicular network," *IEEE Open Journal of the Communications Society*, vol. 2, pp. 687–703, 2021.
- [8] C. You, B. Zheng, and R. Zhang, "Wireless communication via double irs: Channel estimation and passive beamforming designs," *IEEE Wireless Communications Letters*, vol. 10, no. 2, pp. 431–435, 2021.
- [9] Z. Li, M. Hua, Q. Wang, and Q. Song, "Weighted sum-rate maximization for multi-irs aided cooperative transmission," *IEEE Wireless Communications Letters*, vol. 9, no. 10, pp. 1620–1624, 2020.
- [10] H. Niu, Z. Chu, F. Zhou, C. Pan, D. W. K. Ng, and H. X. Nguyen, "Double intelligent reflecting surface-assisted multi-user mimo mmwave systems with hybrid precoding," *IEEE Transactions on Vehicular Technology*, vol. 71, no. 2, pp. 1575–1587, 2022.
- [11] X. Ma, Y. Fang, H. Zhang, S. Guo, and D. Yuan, "Cooperative beamforming design for multiple ris-assisted communication systems," *IEEE Transactions on Wireless Communications*, vol. 21, no. 12, pp. 10 949–10 963, 2022.
- [12] D. Kumar, J. Kaleva, and A. Tölli, "Blockage-aware reliable mmwave access via coordinated multi-point connectivity," *IEEE Transactions on Wireless Communications*, vol. 20, no. 7, pp. 4238–4252, 2021.
- [13] L. Jiao, P. Wang, A. Alipour-Fanid, H. Zeng, and K. Zeng, "Enabling efficient blockage-aware handover in ris-assisted mmwave cellular networks," *IEEE Transactions on Wireless Communications*, vol. 21, no. 4, pp. 2243–2257, 2022.
- [14] G. Zhou, C. Pan, H. Ren, K. Wang, M. Elkashlan, and M. D. Renzo, "Stochastic learning-based robust beamforming design for ris-aided millimeter-wave systems in the presence of random blockages," *IEEE Transactions on Vehicular Technology*, vol. 70, no. 1, pp. 1057–1061, 2021.
- [15] M. A. L. Sarker, M. Baek, and D. S. Han, "Blockage-aided ris cooperative joint beamforming for mmwave mimo systems," *IEEE Transactions on Vehicular Technology*, vol. 73, no. 1, pp. 1406–1411, 2024.
- [16] Y. Yang, S. Dang, M. Wen, B. Ai, and R. Qingyang Hu, "Blockage-aware robust beamforming in ris-aided mobile millimeter wave mimo systems," *IEEE Transactions on Wireless Communications*, vol. 23, no. 11, pp. 16 906–16 921, 2024.
- [17] I. Hemadeh, A. Y. Tsai, P. Svedman, D. G. Jagyasi, K. J.-L. Pan, T. Cogalan, G. Zhang, and A. Shojaeifard, "Reconfigurable intelligent surfaces (ris) aided initial access," US Patent Application 2025/0202539 A1, 2025, application No. 18/849,787, Filed Apr 3, 2023, Published Jun 19, 2025, Assignee: InterDigital Patent Holdings, Inc.
- [18] Q. Shi, M. Razaviyayn, Z.-Q. Luo, and C. He, "An iteratively weighted mmse approach to distributed sum-utility maximization for a mimo interfering broadcast channel," *IEEE Transactions on Signal Processing*, vol. 59, no. 9, pp. 4331–4340, 2011.
- [19] D. Brandwood, "A complex gradient operator and its application in adaptive array theory," *IEE Proceedings F (Communications, Radar and Signal Processing)*, vol. 130, pp. 11–16, 1983.